

Meso-Structure Formation for Enhanced Organic Photovoltaic Cells

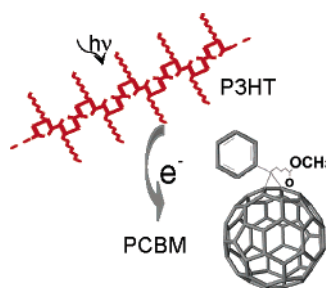
Marisol Reyes-Reyes,^{†,‡} Kyungkun Kim,[†] James Dewald,[§]
Román López-Sandoval,^{||} Aditya Avadhanula,[§] Seamus Curran,[§] and
David L. Carroll^{*,†}

Center for Nanotechnology and Molecular Materials, Department of Physics, Wake
Forest University, Winston-Salem, North Carolina 27109, Instituto de Investigación en
Comunicación Óptica, Universidad Autónoma de San Luis Potosí, Alvaro Obregón 64,
San Luis Potosí, Mexico, IPCYT Advanced Materials Department, Department of
Physics, San Luis Potosí, Mexico, and New Mexico State University,
Las Cruces, New Mexico

carrolldl@wfu.edu

Received August 12, 2005

ABSTRACT



Formation of a controlled fullerene mesophase within an organic host system has enabled us to create high-power conversion efficiency photovoltaics. This mesophase is formed using thermal gradients that provide a fluidic mobility of the fullerenes allowing for greater dispersion of nanocrystalline 1-(3-methoxycarbonyl)propyl-1-phenyl-(6,6)C₆₁ (PCBM) within regioregular poly(3-hexylthiophene) (P3HT). From this reorganization of the component materials in the matrix the overall efficiency of the system jumps dramatically from the roughly 2.4% to 5.2%.

A “grand challenge” of the nanosciences, in particular for organic-based materials, is frequently identified as the creation of an ordered nanophase that extends over many microns. These are also referred as “scaled structures” or “hierarchical structures” because there is structure found at many different length scales in them. This placement of nanomaterials into three-dimensional arrays is thought to provide a way of engineering novel super materials at the macroscale.^{1,2}

As is well-known, polymer photovoltaics promise flexibility and high efficiency through excellent absorption cross-

sections for use in solar cells.^{3–5} However, they suffer from a severe mismatch in length scale, strong fluorescence, and morphological control. Typically, it is desired to disperse nanostructured interfaces throughout the bulk of absorbing material such that the excitons are efficiently separated into electrons and holes before recombination.^{6,7} The best known nanomaterial to create such “bulk heterojunctions” is the

(2) Tosheva, L.; Valtchev, P. V. *Chem. Mater.* **2005**, *17*, 2494.

(3) Shaheen, S. E.; Ginley, D. S.; Jabbour, G. E. *MRS Bull.* **2005**, *30*, 10.

(4) Forrest, S. R. *MRS Bull.* **2005**, *30*, 28.

(5) Janssen, R. A. J.; Hummelen, J. C.; Sariciftci, N. S. *MRS Bull.* **2005**, *30*, 33.

(6) Shaheen, S. E.; Brabec, C. J.; Sariciftci, S.; Padinger, F.; Fromherz, T.; Hummelen, J. C. *Appl. Phys. Lett.* **2001**, *78*, 841.

(7) van Duren, J. K. J.; Yang, X.; Loos, J.; Bulle-Lieuwma, C. W. T.; Sieval, A. B.; Hummelen, J. C.; Janssen, R. A. J. *Adv. Funct. Mater.* **2004**, *14*, 425.

[†] Wake Forest University.

[‡] Universidad Autónoma de San Luis Potosí.

^{||} IPCYT Advanced Materials Department.

[§] New Mexico State University.

(1) Cao, A.; Veedu, V. P.; Li, X.; Yao, Z.; Ghasemi-Nejhad, M. N.; Ajayan, P. M. *Nature Mater.* **2005**, *4*, 540.

fullerene and its derivatives. Since the hole is typically the high mobility carrier, in the regioregular P3HT case,⁸ enhancing electron mobility further serves to provide charge balance to devices. While this has worked well, the hopping nature of electrons in sub-percolating networks of fullerenes severely limits the maximum obtainable efficiency. What is needed is control over the structure of the nanophase that will allow for tailored carrier mobilities. To control the mesophase, we have attempted to create single crystalline nanowhiskers of PCBM pointing toward the cathode (but not touching it) from the anode. This provides an increase in the electron mobility more closely matching that of the holes in the P3HT. We demonstrate this mesophase control in the P3HT:PCBM system, famed for its possible applications to organically based solar cells.^{9–12}

The standard device used in these studies is built by spin casting poly(3,4-ethylenedioxythiophene):poly(styrenesulfonate) (PEDOT:PSS) (Baytron P) onto cleaned ITO substrates (Delta Technologies $R_s = 10 \text{ Ohm square}^{-1}$). The PEDOT:PSS layer is approximately 80 nm thick. A blend of regioregular P3HT (Aldrich: regioregular with an average molecular weight, $M_w = 87 \text{ kg mol}^{-1}$, without further purification) and PCBM (American Dye Source) is then spin coated onto the PEDOT layer. Subsequently, a LiF (0.3–0.4 nm) and Al (80 nm) cathode is evaporated onto the polymer stack. This device is removed from the evaporator and encapsulated using glass capsules with a silicon seal. Once the devices are built and encapsulated, the device is annealed on a hot plate. Performance of the devices was determined using a calibrated AM1.5 G solar simulator (Oriel) at 80 mW cm^{-2} illumination. Current voltage curves were obtained using a standard source measurement unit (Keithley SMU) from which the maximum power rectangle was determined. From this the fill factor and efficiency of the device was calculated.

To optimize the device before annealing, the ratio of polymer to PCBM was determined by varying from 1:1 (polymer to PCBM) to 1:0.46 for two different thicknesses of P3HT films. The maximum efficiency was obtained at a surprisingly low loading of PCBM for both the thick (about 170 nm) and thin (about 120 nm) films shown in Figure 1a. Next, the optimally loaded devices were annealed (shown in Figure 1b) to create ordering (crystallization) within the nanophased materials (P3HT). The devices were annealed to 155°C for different lengths of time to determine the maximum efficiency that could be obtained.¹² We note that lower temperatures were also investigated and it was found that 155°C was the optimal annealing window to provide significant mobility to the PCBM phase. Annealing between two and three minutes results in efficiencies around 5.2%.

(8) Pandey, S. S.; Takashima, W.; Nagamatsu, S.; Endo, T.; Rikukawa, M.; Kaneto, K. *Jpn. J. Appl. Phys.* **2000**, *39*, 94.

(9) Padinger, F.; Rittberger, R. S.; Sariciftci, N. S. *Adv. Funct. Mater.* **2003**, *13*, 85.

(10) Schilinsky, P.; Waldauf, C.; Brabec, C. J. *Appl. Phys. Lett.* **2002**, *81*, 3885.

(11) Chirvase, D.; Parisi, J.; Hummelen, J. C.; and Dyakonov, V. *Nanotechnology* **2004**, *15*, 1317.

(12) Reyes-Reyes, M.; Kim, K.; Carroll, D. L. *App. Phys. Lett.* **2005**, *87*, 083506.

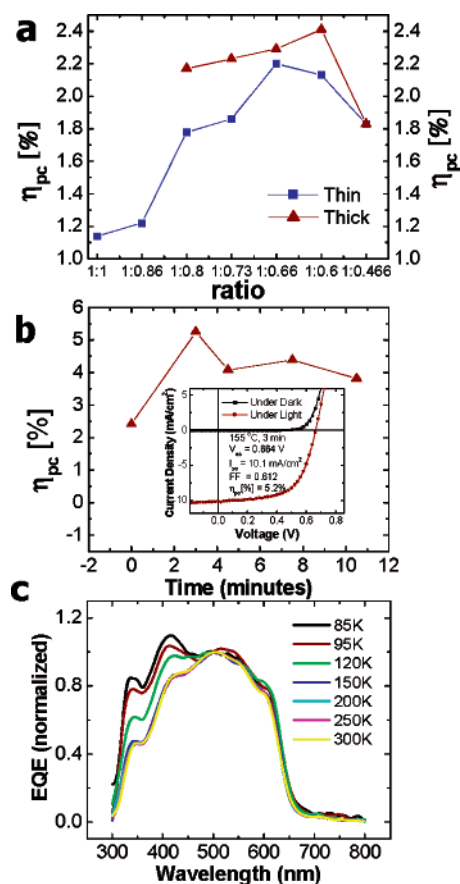


Figure 1. (a) Power conversion efficiency (η_{pc}) for different loading of PCBM to P3HT for thin (square symbols) and thick (triangle symbols) unannealed active layer. (b) Influence of the annealing time at 155°C on power conversion efficiency. Inset of (b) shows J–V curves at 3 min in the dark and under white light illumination (80 mW cm^{-2}). (c) External quantum efficiency (EQE) as a function of incident wavelength for the annealed (155°C at 3 min) active layer of ITO/PEDOT:PSS/P3HT:PCBM/LiF/Al heterojunction.

This is an enhancement of more than 120%. We note that continued annealing at this temperature or lower, results in an overall degradation of the device performance. In the inset of Figure 1b we show the current density–voltage curves at the optimal loading (155°C by 3 min), under white light illumination the values V_{oc} , I_{sc} , and FF are showed.

An examination of electron conduction mechanisms within the active layer shows that there is a change in the mesophase due to annealing. Figure 1c shows the external quantum efficiency (EQE) as a function of incident wavelength for temperatures between 80 and 300 K. Generally, the feature related to fullerene absorption occurs at 350 nm, and the 500 nm feature is related to the polymer. Notice that the fullerene feature grows rapidly compared to the polymer features suggesting crystalline conductivity is now occurring in the mesophase. On the other hand, the same EQE study as a function of the temperature has been realized for the unannealed sample (not shown). In this case, we do not observe the increasing of the fullerene to polymer feature

ratios when we lower the temperature. This suggests that relatively low hopping conductivity is occurring in the fullerene component in the annealed case relative to the unannealed devices indicating that mesophase crystals extend across the P3HT layer.

This ordering of the mesophase is accompanied by a corresponding change in the absorption and luminescence of the active layer. Figure 2a compares the absorption of

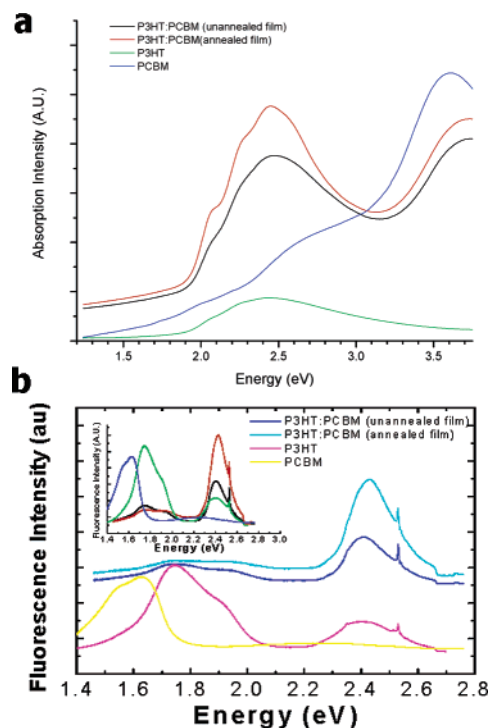


Figure 2. (a) Absorption and (b) fluorescence spectra of PCBM, P3HT, PCBM:P3HT unannealed blend, and PCBM:P3HT annealed blend of the active layer. Inset of (b) shows the comparison between the different fluorescence spectra.

PCBM, P3HT, PCBM:P3HT unannealed blend, and PCBM:P3HT annealed blend. Clearly the absorption features of the pristine materials are not reflected in a simple amalgam of the spectra from blends. The blended samples show an overall absorption red-shift as compared to their pristine states, which suggests that there is a close interaction between PCBM and P3HT. This is a consequence of the mixing of the electronic wave functions and the potential formation of a charge-transfer complex.¹³ The peak at 3.6 eV is from PCBM, and is not effected upon annealing. However, we can see that the P3HT absorption between 2 and 3 eV changes significantly. More significant is that the large absorption increase between 2 and 3.5 eV shows a spectral increase in absorption by 14% due to the annealing. This suggests that the device efficiency enhancement is caused in part by the increase in the overall absorption.

Conjugated systems such as polymers will have their substantial photoluminescence quenched in the presence of

C₆₀ or fullerene derivatives such as PCBM. Fluorescence spectra were obtained using a Renishaw InVia Raman spectrometer equipped with a Raman Leica RE02 microscope, the excitation source being the Ar ion laser at 457 nm. Figure 2b shows that the P3HT fluorescence which is strongest in the infrared, is substantially quenched by being blended with PCBM. In addition, there is a shift of the PI_{max} in the infrared toward the blue also indicating exciton scavenging by the PCBM. Additionally, the PCBM which fluoresces quite strongly in the near-infrared, has its fluorescence completely quenched. When we examine the two blended structures, while the spectra are as expected quite similar, the fluorescence is also reduced when we anneal the samples which would indicate quenching sites and enhanced exciton extraction from the more ordered and closer packed structure. However, there is a fluorescence in the P3HT from the unannealed spectrum (in the IR) and this has been even further reduced (inset of Figure 2b). This has to do with a greater interaction between the PCBM and its ability to enhance electron transfer due to mesophase changes.

This is further reflected on the nanoscale as seen in NSOM. The AFM/NSOM images shown in Figure 3 were obtained

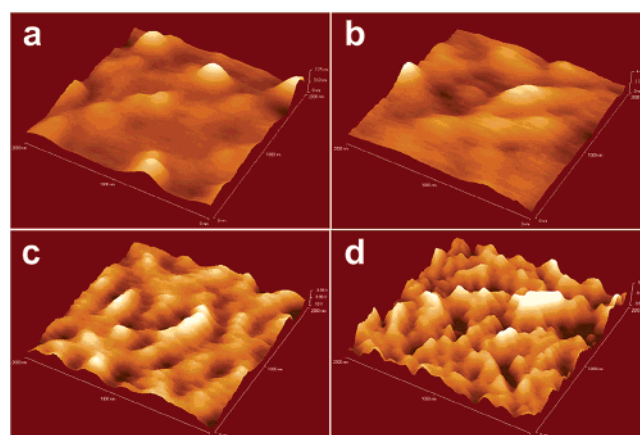


Figure 3. AFM (a, b) and NSOM (c, d) images of the unannealed (a, c) and annealed (b, d) active layer.

using a Veeco Aurora3 near-field scanning optical microscope (NSOM). Thin films of the nanocomposites were spun cast onto a glass cover, and the film was imaged using the near-field scanning optical microscope in transmission mode using a 457 nm Ar ion laser. However, since both the P3HT and the PCBM phases absorb at our lumination wavelength, the light at the NSOM tip is primarily fluorescence from the P3HT phase. Further, topographical as well as optical transmission images were obtained simultaneously.

NSOM analysis shown in Figure 3c,d of the two composite films reveals more insight into the ordering and structure of the composite. Both annealed (Figure 3a) and unannealed (Figure 3b) films are almost completely flat with a variation in topography of only 4 nm across a few microns. We can

(13) Mulliken, R. S. *J. Am. Chem. Soc.* **1952**, 74, 811.

see, however, that there are substantial differences in the optical signal, as the “spiked” structures would suggest regions of greater fluorescence that correlate to areas without the fullerenes. This is because the fullerene clusters separate the excitons, thereby quenching the fluorescence, and thus those regions appear slightly darker. This is shown in Figure 3c (unannealed film) and Figure 3d (annealed film). The unannealed samples show large regions of quenching, which would suggest large aggregates of the PCBM varying in sizes from a few 10's of nm to 100's of nm. We note that this does not necessarily mean that such aggregates are crystalline, only that there is a high density of PCBM in these regions. However, after annealing, we see that there is a much finer detail in quenching across the film, suggesting a greater dispersion of the PCBM dense region. The better dispersion of PCBM nanocrystals ensures that there is a more efficient PCBM:P3HT interaction, a greater surface area for interaction, and subsequently we get better luminescence quenching with the consequence of improved exciton disassociation. The NSOM is not sensitive to the overall phase of the P3HT/PCBM and we cannot determine whether the PCBM has become more crystalline from these images. However, crystallization of the PCBM phase is clearly playing a significant role in the overall performance enhancement as shown from Figure 1c. It is important to note that crystallization of the P3HT must also be occurring as has been reported by several authors.^{9,11} This undoubtedly leads to higher mobilities in hole transport. We know that such crystallization properties of the host P3HT will depend on the concentration of PCBM. Thus, we conclude that crystallization in both phases, for these low loadings of PCBM, compliment charge balance within the device.

By analyzing the conduction curves as a function of temperature (not shown), the energy associated with hopping conduction was determined to be roughly 31 meV for unannealed and 24 meV for annealed samples. If the overall dispersion of the individual fullerenes was increased under annealing, meaning there was significant distance between each balls, then we would expect the energy for hopping to increase. This did not happen, suggesting that the pathways for percolating conduction are becoming more crystalline. Large crystals were not observed in transmission electron microscopy imaging however (see Figure 4). This means that these small “crystalline” pathways are well dispersed throughout the matrix. This has already been suggested by Yang et al.^{14–15} The existence of these PCBM nanocrystals were corroborated by using high-resolution transmission microscopy (HRTEM, JEOL 2010 FEG FASTEM operated at 200 kV). We have observed a great difference in the morphology

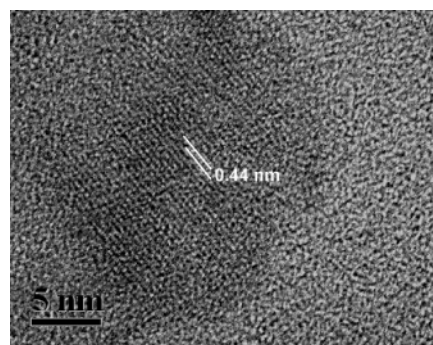


Figure 4. HRTEM image of PCBM nanocrystal in P3HT host after annealing at 155 °C by 3 min in the active layer.

of PCBM before and after annealing. In the first case, we have not observed the formation of PCBM nanocrystal. In the second one, we have found the formation of small PCBM crystal (Figure 4). The d spacing in these PCBM crystals is about 0.44 nm in accordance with the result found by Yang et al.¹⁶

We note further that if the nanocrystals were oriented parallel to the contacts, hopping conduction would still be significant. This suggests that some order, perpendicular to the contacts, must exist, reducing the overall resistance to current flow out of the device. Though this is not direct proof, it is suggestive of the overall morphology of the nanophase. It is surprising to suggest that the annealing process has produced alignment within the crystallites. Indeed, PCBM crystal formation might be expected to occur homogeneously within the polymer host.

In summary, the results suggest an oriented crystalline morphology of PCBM in the conjugated matrix using surprisingly low concentrations of PCBM. In our devices, this alteration in the mesophase leads to better ordering and dispersion of PCBM nanocrystals. We suggest the thermal treatment allows for a pseudofluidic state to exist in which P3HT and PCBM are allowed to rearrange into crystalline nano-domains. This control over the morphology allows a sensitive handle with which to achieve high mobility charge balance, increasing the overall efficiency of the device.

Acknowledgment. This work was supported at Wake Forest University by the Air Force Office of Sponsored Research (AFOSR) under Grant No. FA9550-04-1-0161, at New Mexico State University by EPSCoR NSF Grant No. 0132632, and at IPICYT by CONACYT Mexico through Grant No. J-41452.

OL051950Y

(14) Yang, X.; Alexeev, A.; Michels, M. A. J.; Loos, J. *Macromolecules* **2005**, *38*, 4289.

(15) Yang, X.; Loos, J.; Veenstra, S. C.; Verhees, W. J. H.; Wienk, M. M.; Kroon, J. M.; Michels, M. A. J.; Janssen, R. A. J. *Nano Lett.* **2005**, *5*, 579.

(16) Yang, X.; van Duren J. K. J.; Rispen, M. T.; Hummelen, J. C.; Janssen, R. A. J.; Michels, M. A. J.; Loos, J. *Adv. Mater.* **2004**, *16*, 802.